Proceedings of the 18th World Congress
The International Federation of Automatic Control
Milano (Italy) August 28 - September 2, 2011

Water Management in PEM Fuel Cells: Controllability Analysis and Steady-state Optimization for Temperature Control

Alicia Arce * **Carlos Bordons** * **Alejandro J. del real** *

* *Automation and System Engineering Department, University of Seville, 41092 Sevilla, Spain. (e-mails: aarce@cartuja.us.es, bordons@esi.us.es, adelreal@cartuja.es).*

Abstract: This paper presents a controllability study of the water management inside anode channel by regulating the stack temperature for PEM fuel cell systems with dead-ended anode. Moreover, this work includes the design of a steady-state target optimizer which calculates the temperature set-point profiles that minimize the stack degradation and the hydrogen leaks. The control architecture is successfully simulated and the results show promising performance.

Keywords: Thermal degradation, optimal operation and control of power systems, model predictive and optimization-based control.

1. INTRODUCTION

Fuel cell systems are considered to be feasible candidates to replace the conventional energy conversion systems for stationary and mobile applications. Specifically, this work is focused on Polymeric Electrolyte Membrane (PEM) fuel cells since they present appropriate properties such as fast start-up, high energy density and low operation temperature for aforementioned applications. However, this technology presents some drawbacks that must be overcome in order to become competitive. One of the more relevant drawbacks is the fast degradation rate and consequently the short fuel cell lifespan. It is observed in dead-ended anode fuel cell systems that the liquid water content inside the anode channel is strongly related to temporal and permanent degradation processes such as flooding and corrosion phenomena. Therefore, in this paper the influence of the stack temperature on the liquid water management is studied with the objective of proposing a temperature control technique to optimally regulate the liquid water content inside the anode channel.

In the literature, few papers such as Karnik et al. (2009); Chen and Peng (2004) deal with the control of water management by regulating the humidity of the reactants and the purges cycles. However, to the best of the authors' knowledge, these works disregard the relation between the stack temperature and the liquid water management inside the fuel cell system. Otherwise, there are several works such as Ahn and Choe (2008); Riascos and Pereira (2009); Na and Gou (2008) which study the control temperature of fuel cell systems and as previously mentioned there is again no direct connection between stack temperature and water management. The work presented by Siegel and Stefanopoulou (2009) develops a hybrid model of the water distribution inside the gas diffusion layer (GDL) and channels which relates the evaporation and condensation processes to the one-dimensional spatial distribution of the water inside the anode. For the sake of simplicity the studies presented in this work are based on an fuel cell model published in del Real et al. (2007) which accounts for liquid water dynamics neglecting its spatial distribution.

This work first presents a study of the liquid water management controllability by regulating the stack temperature. Then, a control architecture based on a steady-state target optimizer is proposed in order to control the liquid water inside the anode channel. The paper is organized as: Section 2 summarizes the fuel cell model which is the basis of the study presented in this work. In Section 3, the liquid water management controllability is studied in detail. Section 4 proposes a control architecture in order to control the stack temperature and Section 5 shows the simulation results. Lastly, Section 6 discusses the conclusions of this work.

2. FUEL CELL MODEL

As mentioned in the introduction this work is based on the fuel cell model previously published in del Real et al. (2007). The fuel cell system under study is manufactured by Ballard and supplies as a maximum power 1.2 kW and comprises 46 cells each with a 110 cm^2 membrane. The fuel cell model is semi-empirical and zero-dimensional and includes thermal dynamics, two-phase water dynamics and the effects of the flooding phenomenon on the stack voltage.

The thermal equations are summarized in this section. The physical parameters have been obtained experimentally from the data of the bed-test installed at the University of Seville facilities. An energy balance is performed in order to obtain the thermal model, accounting for the energy rate produced in the chemical reaction of water formation (which is supposed to be formed as water vapor), $\dot{H}_{reac}$, the power supplied in the form of electricity, P_{st}, and the amount of heat evacuated by radiation, $\dot{Q}_{rad,FC2amb}$, and both natural and forced convection,

[1] This work was supported by Spanish Ministry of Science and Innovation under grant DPI2008-05818.

$\dot{Q}_{conv,FC2amb}$. Heat removal is completed through forced convection by a fan. The energy balance results in:

$$m_{st} \cdot C_{st} \cdot \frac{dT_{st}}{dt} = \dot{H}_{reac} - P_{st} - \dot{Q}_{rad,FC2amb} - \dot{Q}_{conv,FC2amb} \quad (1)$$

The heat transfer dynamics of the fuel cell are several magnitude orders slower than the fluid-dynamics associated with the cooling air flow, therefore, the last ones are neglected in our model. Moreover, the amount of air supplied by the fan can be considered as linearly proportional to the control signal of the fan. In this way, the equation that links the fan voltage, V_{fan}, between 0 and 100 (%), with the air flow supplied expressed in kg s^{-1}, $\dot{m}_{cool}$, is given by:

$$\dot{m}_{cool} = 36 \cdot V_{fan} \ . \quad (2)$$

The thermistor can be modeled by a first-order approximation with a time constant of 10 seconds.

$$\tau \cdot \frac{dT^*_{st}}{dt} + T^*_{st} = T_{st} \ , \quad (3)$$

where T^*_{st} is the temperature measured by the thermistor and τ is the time constant of the thermistor.

With respect to the fluid-dynamics equations, five control volumes are considered, rather than nine as in the case of McKay et al. (2005), in order to reduce the computational cost of the model, while still accounting for all of the effects presented in that model. Moreover, unlike previous work, the effects of water evaporation and condensation dynamics are explicitly considered in our model. The fluid-dynamics block is composed of five interconnected sub-blocks, which correspond to, the control volumes of the two flow channels, the diffusion gas layers of cathode and anode and the transport of chemical species across the membrane. Each of these control volumes are assumed to be at a temperature equal to that of the stack, T_{st}. The equations of each control volumes are detailed in del Real et al. (2007). The assumptions considered in this model related to the water accumulation inside the anode channel are validated by comparing the stack voltage drop caused by the phenomenon referred to as flooding.

The successful validation of this model with experimental data is presented in del Real et al. (2007). Therefore, it is assumed that this model is suitable for the design of control architectures related to water management.

3. STUDY OF THE SYSTEM CONTROLLABILITY

In order to study the controllability of this problem it is important to remark that the fuel cell system under study is cooled down by an air fan and the water accumulation inside the anode channel strongly depends on the stack current and temperature. The stack current is considered in this work as a measurable disturbance and therefore the temperature is the only controllable variable in order to regulate the liquid water inside the anode channel. The purge valve is incorporated to the fuel cell system in order to remove the water inside the anode channel when the voltage drop reaches certain values. The controllability is studied by determining the maximum temperature curve, the curve of the temperatures which compensate the amount of water dragging to the anode channel with the water evaporation, and the minimum temperature curve. The maximum temperature curve corresponds to the temperature limits provided by the supplier's datasheet due to the thermal stress of the membrane. With respect to the curve of the temperatures which compensates the evaporation and water dragging, these temperatures correspond to zero water flow inside the anode channel, that is, the slope of the curve of the water mass inside the anode channel equal to zero. The steady-state surface of the water flow inside the anode channel varying the stack current and temperature is obtained by simulating the fuel cell model considering the air pump regulated by the controller proposed in Arce et al. (2010) and the air fan manipulated by a local controller developed in Arce et al. (2011). Figure 1 shows the resulting surface and the interception with the XY-plane which corresponds to the compensation temperatures.

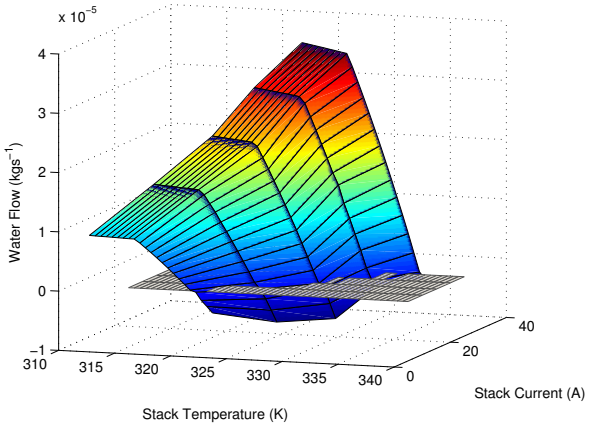

Fig. 1. Steady-state liquid water flow against stack temperature and current

The Extremum Seeking Algorithm (ESA) is proposed in order to obtained the compensation temperatures for the overall range of current. ESA is a local minimum algorithm which is used in real-time optimization, control and parametrization. In general, this method does not rely on a model for the optimization and it is considered as a non-linear on-line optimization algorithm for unconstrained problems. Recently, few papers such as O'Rouke et al. (2009); Chang and Moura (2009) deal with the optimization control for fuel cell system proposing ESA as solution. In both papers, the algorithm has been successfully implemented for regulating the air supply. In contrast, the algorithm proposed in this paper seeks the minimum of the square function of the water flow for different stack currents.

3.1 Extremum Seeking Algorithm formulation

This problem is solved as a minimization of a function of one variable which is closely related to solving one non-linear equation with one unknown as explained in Dennis and Schnabel (1996). After studying the steady-state curves of the fuel cell system, the existence and uniqueness of a solution for each stack current (considered as measurable disturbance) are guaranteed. The local minimum of a continuously differentiable function must come at a point where $f'(x) = 0$. Graphically, this is interpreted as saying that the function cannot initially increase in either direction from this point.

The algorithm which has been implemented is based on the increment of the stack temperature. The fuel cell system is run until the steady-state is reached, then the slope of the water mass inside the anode channel is measured. The next step

change of the design variable is calculated using the gradient as shown in the following equation:

$$T_{st}(k+1) = T_{st}(k) + H_{esa} \cdot \frac{\dot{m}_{l,anch}(k) - \dot{m}_{l,anch}(k-1)}{T_{st}(k) - T_{st}(k-1)}, \quad (4)$$

where, $T_{st}(k+1)$ is the next step value of the stack temperature, $T_{st}(k)$ is the steady-state value of stack temperature in the current algorithm iteration, $T_{st}(k-1)$ is the steady-state value of the stack temperature in the previous algorithm iteration, H_{esa} is the tuning gain factor, $\dot{m}_{l,anch}(k)$ is the steady-state value of the slope of the water mass for the current iteration and its tuning is done by heuristic techniques, and $\dot{m}_{l,anch}(k-1)$ is the steady-state value of the slope of water mass for the current iteration. In this study, it is assumed that the fuel cell is perfectly controlled, therefore the design variable is the stack temperature instead of the air fan voltage which is the variable which can be actually manipulated. The scheme of the Extremum Seeking Algorithm implemented on the fuel cell model is presented in Figure 2. The algorithm stops the simulation when the derivative of the

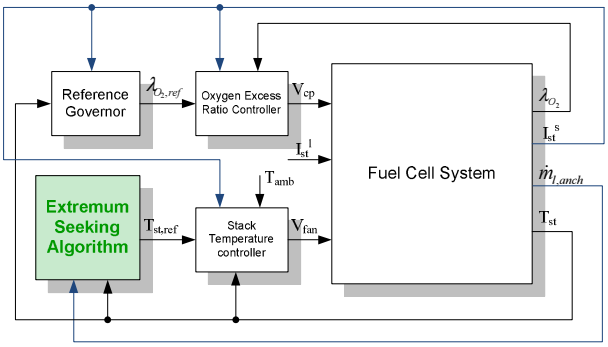

Fig. 2. Extremum Seeking Algorithm block diagram

water flow is sufficiently close to zero which is determined by a threshold and is repeated for a range of load currents from 2 A to 35 A.

3.2 Results and discussion

The ESA algorithm is performed on the non-linear model since the real-time implementation on the real plant might dry the membrane and permanently damage the fuel cell stack. Figure 3 shows the stack temperature, T_{st}, and the water flow inside the anode channel, $\dot{m}_{l,anch}$, resulting of simulating various stack currents. As can be observed, the water flow converges to zero for all the stack currents while the stack temperature tends to the value referred to as compensation temperature. It is clear to see that the higher current the higher compensation temperature. The reason is that the accumulation of water inside the fuel cell is higher for higher stack current demands and thus, the flow of water dragged to the anode channel is higher, the amount of water which has to be evaporated is greater and the compensation temperature raises.

Once the compensation temperatures are obtained, the controllability of the water accumulation is studied by representing the maximum temperatures provided by the supplier due to thermal stress of the membrane and the compensation temperature curve. Figure 4 presents both curves and also includes the minimum temperature curve. The minimum temperature curve is defined by the temperatures presented in Figure 1 which divides the surface in two different slope regions. Lower temperatures than the minimum temperature have small water flow variation

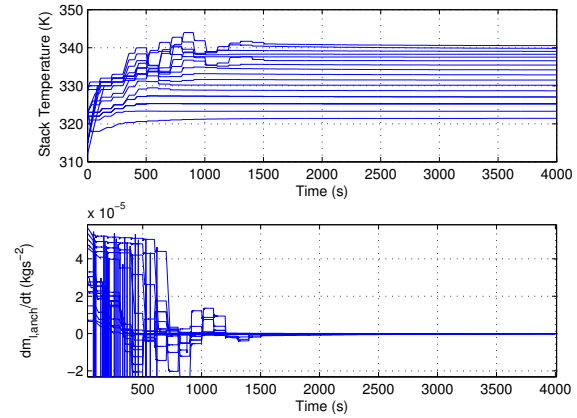

Fig. 3. Extremum Seeking Algorithm simulations

and increase the period of time to reach the water flow set-point due to the fact that the temperature dynamic is very slow. Moreover, the controllability regions are shown in Figure 4. For stack currents lower than 20 A, the maximum temperature is higher than the compensation temperature and the water content can be regulated. Otherwise, for stack current higher than 20 A, the compensation temperature is over the maximum bound imposed by the supplier and therefore, the water content inside the anode cannot be controlled by regulating the stack temperatures and anode purges are required to remove it.

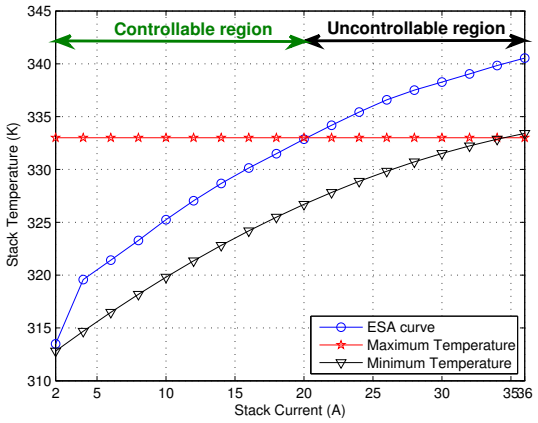

Fig. 4. Controllability regions

4. CONTROL DESIGN

The scheme of the control architecture proposed in this work to regulate the liquid water inside the anode channel is shown in Figure 5 where different control levels are represented. The lower control level corresponds to the block referred to as local controller which is proposed to be a model predictive controller but the design of this controller is not the scope of this study (Arce et al. (2011)). The goal of the local controller is to regulate the fan voltage in order to track a temperature set-point. In a higher control level, a steady-state target optimizer is included to obtain a prediction of the future temperature profile. This temperature profile minimizes the quadratic difference between the water content inside the anode channel and a certain value suitably chosen subject to degradation constraints.

Moreover, observers are required to estimate variables which cannot be directly measured by the sensors available at the laboratory setup.

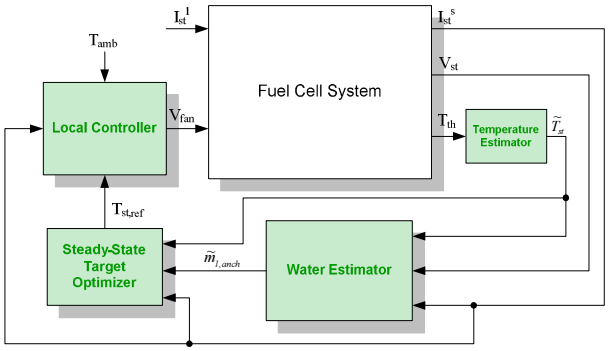

Fig. 5. Control architecture

4.1 Estimators

The observers simplify the fuel cell model presented in Section 2 for real-time implementation purposes. The variables which are required to be estimated are the stack temperature and the liquid water accumulation inside the anode. The stack temperature is estimated by the temperature measurements of a thermistor and the water content is observed by the measurements of the stack current, stack temperature and stack voltage. In the present paper, the closed-loop observer of the water content is detailed.

The water mass inside the anode is the integration of the water flow inside the anode channel which is shown in Figure 1. The water flow, $\dot{m}_{l,anch}$, is function of the stack temperature, T_{st}, and the stack current, I_{st}^s, assuming reactant flows and humidities are perfectly controlled. Specifically, this function can be expressed as a piece-wise affine linear function of the temperature in two regions where the coefficients are quadratic function of the stack current in turn. Both regions are limited by the defined minimum temperature, T_{min}. Therefore, the water flow estimation is:

$$\tilde{m}_{l,anch} = \begin{cases} a_1(I_{st}^s)\ T_{st} + b_1(I_{st}^s)\ \ if\ T_{st} \le T_{min}(I_{st}^s) \\ a_2(I_{st}^s)\ T_{st} + b_2(I_{st}^s)\ \ if\ T_{st} > T_{min}(I_{st}^s) \end{cases} , \quad (5)$$

where

$$a_1 = -6.13\ 10^{-11}\ (I_{st}^s)^2 - 1.32\ 10^{-8}\ I_{st}^s + 9\ 10^{-9} , \quad (6)$$
$$b_1 = 2.06\ 10^{-8}\ (I_{st}^s)^2 + 5.8\ 10^{-6}\ I_{st}^s - 2.81\ 10^{-6} , \quad (7)$$
$$a_2 = 3.06\ 10^{-9}\ (I_{st}^s)^2 - 2.89\ 10^{-7}\ I_{st}^s - 4.32\ 10^{-7} , \quad (8)$$
$$b_2 = -9.48\ 10^{-7}\ (I_{st}^s)^2 + 9.60\ 10^{-5}\ I_{st}^s + 0.000118 . \quad (9)$$

The accumulation of water inside the anode channel is equal to the integral of the water flow:

$$\tilde{m}_{l,anch} = \int_0^t \tilde{m}_{l,anch}(\tau)\ d\tau . \quad (10)$$

The closed-loop observer is formulated as:

$$\tilde{m}_{l,anch} = \int_0^t \tilde{m}_{l,anch} d\tau + K\ (V_{st} - \tilde{V}_{st}) , \quad (11)$$

being K the weighting factor of the estimation of the voltage and $\tilde{V}$ is the stack voltage estimation which is defined as presented in del Real et al. (2007):

$$\tilde{V}_{st} = n_{fc}\ \big(x_1 + x_2\ (T_{st} - 308) + x_3\ \big(0.5\ ln(\tilde{p}_{O_2,cach}) + \\ + ln(\tilde{p}_{H_2,anch})\big) - x_4\ (1 - e^{-\tilde{j}/x_5}) - x_6\ \tilde{j} - \\ - x_7\ \tilde{j}^{1+x_8}\big) , \quad (12)$$

where

$$\tilde{j} = \frac{I_{st}^s}{A_{fc}^0\ (1 - \alpha_l\ \tilde{m}_{l,anch})} . \quad (13)$$

In the same conditions, the oxygen and hydrogen pressures are assumed to be functions of the current and temperature. Specifically, the oxygen pressure, $\tilde{p}_{O_2,cach}$, depends on the stack current, I_{st}^s, and the stack temperature, T_{st}, and the hydrogen pressure, $\tilde{p}_{H_2,anch}$, is function of the stack temperature:

$$\tilde{p}_{H_2,anch} = -1.2621\ 10^{-4}\ T_{st}^2 + 0.076\ T_{st} - 10.149 , \quad (14)$$
$$\tilde{p}_{O_2,anch} = a_3(I_{st}^s)\ T_{st} + b_3(I_{st}^s) . \quad (15)$$

4.2 Steady-state target optimizer

The steady-state target optimizer as presented in Muske (1997) calculates the future temperature profile, $\mathbf{T_{st,ref}}$, with the goal of maintaining the water content inside the anode, $m_{l,anch}$, over a determined value. This steady-state optimizer is based on a quadratic programming (QP) algorithm and is formulated as a predictive control problem based on state-space models. The input of the state-space model is the set-point temperature, the stack current is considered as measurable disturbance and the output is the accumulation of water. Equations (5) and (10) can be discretized by performing Euler method and assuming that the stack current is invariable in the future instants and equal to the value measured by the current sensor in the present instant. So that, the water content can be expressed as:

$$m_{l,anch}(k+1) = a_i\ h\ T_{st}(k) + m_{l,anch}(k) + b_i\ h , \quad (16)$$

where the index, $i = 1,2$, depends on the stack temperature as seen in Section 4.1 and h is the sampling time for the steady-state target optimization. The sampling time for this control level is slower than the sampling time for the local control loop. Manipulating the above equation, it can be reformulated as:

$$\begin{bmatrix} m_{l,anch}(k+1) \\ T_{st}(k) \end{bmatrix} = \overbrace{\begin{bmatrix} 1 & a_2\ h \\ 0 & 1 \end{bmatrix}}^{\mathbf{M}} \cdot \begin{bmatrix} m_{l,anch}(k) \\ T_{st}(k-1) \end{bmatrix} + \\ + \underbrace{\begin{bmatrix} a_2\ h \\ 1 \end{bmatrix}}_{\mathbf{N}} \cdot \Delta T_{st}(k) + \underbrace{\begin{bmatrix} b_2\ h \\ 0 \end{bmatrix}}_{\mathbf{P}} ,$$
$$y = \underbrace{[\,1\ 0\,]}_{\mathbf{Q}} \cdot \begin{bmatrix} m_{l,anch}(k) \\ T_{st}(k-1) \end{bmatrix} , \quad (17)$$

where the state vector, x, is defined as $[\,m_{l,anch}(k)\ \ T_{st}(k-1)\,]^T$. This piece-wise affine model is simplified to only one region corresponding to the coefficients a_2 and b_2 since the compensation temperatures are higher than the minimum temperature for all the operating range. The predictions of the water accumulation are computed as shown in Camacho and Bordons (2004):

$$\mathbf{m_{l,anch}} = \begin{bmatrix} \hat{m}_{l,anch}(t+1|t) \\ \hat{m}_{l,anch}(t+2|t) \\ \vdots \\ \hat{m}_{l,anch}(t+1|t) \end{bmatrix} = \mathbf{F_{opt}}\ \hat{x}(t) + \mathbf{H_{opt}}\ \mathbf{T_{st}} + \\ + \mathbf{f_{opt}} . \quad (18)$$

where $\mathbf{T_{st}} = [\,\Delta T_{st}(t)\ \Delta T_{st}(t+1)\ \ldots\ \Delta T_{st}(t+N_{opt}-1)\,]^T$ is the vector of future control increments, N_{opt} is the optimization horizon which is the same term as the control horizon for the formulation of the model predictive control, $\mathbf{H_{opt}}$ is a block lower triangular matrix with its non-null elements defined by $H_{opt,ij} = QM^{i-j}N$ and matrices $\mathbf{F_{opt}}$ and $\mathbf{f_{opt}}$ are defined as:

$$\mathbf{F_{opt}} = \begin{bmatrix} QM \\ QM^2 \\ \vdots \\ QM^{N_p} \end{bmatrix}, \quad \mathbf{f_{opt}} = \begin{bmatrix} QP \\ QP + QMP \\ \vdots \\ \sum_{i=1}^{N_p} QM^{i-1}P \end{bmatrix}, \tag{19}$$

being N_p the prediction horizon. The future temperature set-points are calculated minimizing the following objective function:

$$J = (\mathbf{H_{opt}}\mathbf{T_{st}} + \mathbf{F_{opt}}\hat{x}(t) + \mathbf{f_{opt}} - \mathbf{m_{l,anch,ref}})^T(\mathbf{H_{opt}}\mathbf{T_{st}} + \\ + \mathbf{F_{opt}}\hat{x}(t) + \mathbf{f_{opt}} - \mathbf{m_{l,anch,ref}}) + \lambda_{opt}\mathbf{T_{st}^T}\,\mathbf{T_{st}}\,, \tag{20}$$

subject to the following constraints:

$$\underbrace{\begin{bmatrix} I_{N_{opt}\times N_{opt}} \\ -I_{N_{opt}\times N_{opt}} \end{bmatrix}}_{\mathbf{R_{opt}}} \mathbf{T_{st}} = \underbrace{\begin{bmatrix} \mathbf{1}\ 333 - \mathbf{1}\ T_{st}(t-1) \\ \mathbf{1}\ T_{min}(I_{st}^s) + \mathbf{1}\ T_{st}(t-1) \end{bmatrix}}_{\mathbf{c}_{opt}}. \tag{21}$$

where λ_{opt} is the weighting factor, $\mathbf{1}$ is an $(N_{opt}\times 1)$ vector of unit component and I represents the identity matrix.

Determination of the water content set-points.- The optimization presented in the previous section minimizes the quadratic difference between the water content and the water set-point. The water set-points should be calculated by considering degradation issues due to the exposition of the membrane to an excess of water, as mentioned St-Pierre et al. (2000), and the membrane dryness produced by an abrupt change of load current demand, I_{st}^l. Precisely, the last issue determines the minimum water accumulation required to avoid the membrane dryness when the stack current drastically changes to the minimum value which is assumed to be 5 A (the minimum current corresponds to the current demand by the ancillary devices when the load current is zero).

Few minimum water accumulation values are presented in Table 1 which has been obtained by simulating the fuel cell model.

Table 1. Minimum accumulation of water inside the anode channel

Stack Current (A)	$\mathbf{m_{l,anch}}$ (kg)	$\Delta\mathbf{V_{st}}$ (V)
10	$1.802\ 10^{-3}$	0.077
15	$2.196\ 10^{-3}$	0.1375
20	$3.096\ 10^{-3}$	0.1895

5. SIMULATION RESULTS AND DISCUSSIONS

The control architecture is tested on the non-linear model before the real-time implementation. The simulator used in this work is Matlab/Simulink^{TR} which runs on a PC platform.

The control level of the steady-state target optimizer is slower than the local controller level and thus, the sampling time chosen for this optimization is 1.6 seconds and the control horizon is 300 samples, that is, 480 seconds of optimization horizon. In addition, the tuning parameter, λ_{opt}, is equal to 0.002.

The performance of the complete control architecture (see Figure 5) is validated by simulating diverse load current profiles. In concrete, we present the simulating results corresponding to a load current profile shown in Figure 6 which is characterized by current steps of 900 seconds (dynamic with order of magnitude similar to heat transfer dynamics) and values range from 0 A to 20 A that are inside the controllable region.

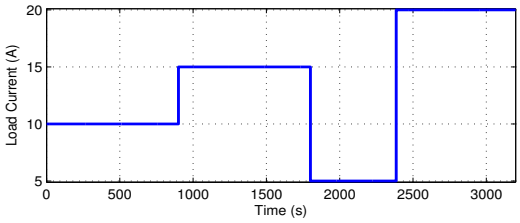

Fig. 6. Load current profile

Figure 7 shows a comparison between the simulation results of the control architecture proposed in this work and the manufacturer's controller with different initial stack temperature conditions. The water content is represented in the top figure and the stack voltage is shown in the bottom figure. As observed in Figure 8, the initial stack temperature for the simulation of the control architecture is 320 K and the manufacturer's controller is simulated for initial stack temperatures of 310 K and 320 K. The water content is influenced by the initial conditions for the case of the manufacturer's controller because the fan voltage is kept constant over a value of 35 % until the stack temperature reaches values closed to the maximum temperature 333 K and then the fan voltage turns to the maximum value, 100 %. As seen in Figure 7, the water accumulation for the case of the manufacturer's controller is regulated by the purge valve while for the proposed control architecture the water content tracks the optimum profile obtained in Section 4.2.1 by means of the temperature controller. For a simulation of 3200 seconds, the anode is purged only one time for our control architecture whereas the manufacturer's controller purges the anode fourteen times. The importance of the minimization of the purges is the reduction of hydrogen leaks which increases the global efficiency. Thus, the control architecture proposed in this work is capable of minimizing the membrane degradation and the hydrogen consumption at the same time. The regulation of the water content influences on the stack voltage performance and consequently on the power supplied by the fuel cell as seen in the bottom plot of Figure 7. The drops of the voltage due to the water accumulation are controlled resulting a higher power supplied by the fuel cell. Note that, for the case of the manufacturer's controller with initial stack temperature of 310 K, the membrane gets dry due to water evaporation around the second 1800 when the load current drastically changes from 20 A to 5 A.

Figure 8 shows the simulation results of the fan voltage and the stack temperature for the case of the proposed control architecture and the manufacturer's controller. In the top figure, the stack temperature is presented with the temperature set-point. The operation of the fan for this case (see the bottom plot) is lower than the case of the manufacturer's controller and thus the net power which is the power supplied by the fuel cell

minus the power consumed by the ancillaries and the global efficiency are higher.

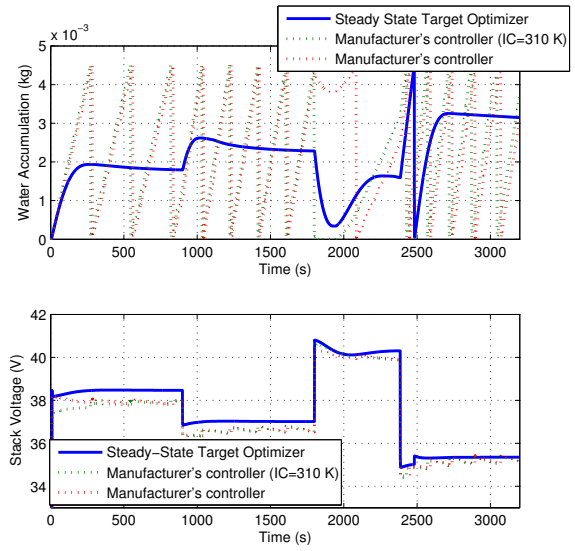

Fig. 7. Simulation results of the water content and stack voltage

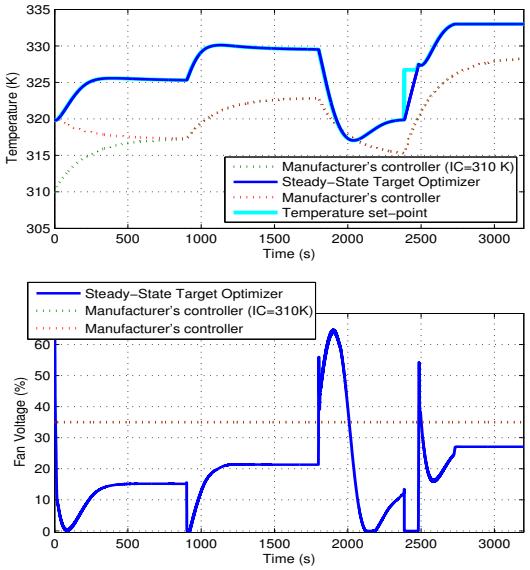

Fig. 8. Simulation results of the stack temperature and fan voltage

The simulations are repeated for faster load current profile, that is, current profile dynamic faster than the heat transfer dynamic. The results show similar behavior than the presented in this section.

6. CONCLUSIONS

This work has presented a study of the controllability of the water management which has shown that the stack temperature can regulate the water inside the anode channel for a certain load current demand. Otherwise, in this paper a steady-state target optimizer has been designed with the objective of minimizing the stack degradation. The simulations have shown promising results but many issues are opened such as the validation of the study with real data, the real-time implementation of the control architecture and the spatial distribution of the temperature along the fuel cell stack.

REFERENCES

Ahn, J.W. and Choe, S.Y. (2008). Coolant controls of a PEM fuel cell system. *Journal of Power Sources*, 179, 252–264.

Arce, A., del Real, A.J., Bordons, C., and Ramirez, D.R. (2010). Real-time implementation of a constrained MPC for efficient airflow control in a PEM fuel cell. *IEEE Transactions on Industrial Electronics*, 57(6), 1892–1905.

Arce, A., Panos, C., Bordons, C., and Pistikopoulos, E.N. (2011). Design and experimental validation of an explicit MPC controller for regulating temperature in PEM fuel cell systems. In *Proceedings of the 18th IFAC World Congress*, in press.

Camacho, E.F. and Bordons, C. (2004). *Model Predictive Control*. Springer–Verlab, London.

Chang, Y.A. and Moura, S.J. (2009). Air flow control in fuel cell systems: An extremum seeking approach. In *Proceedings of the 2009 American Control Conference*.

Chen, D. and Peng, H. (2004). Modeling and simulation of a PEM fuel cell humidification system. In *Proceedings of the 2004 American Control Conference*, 822–827.

del Real, A.J., Arce, A., and Bordons, C. (2007). Development and experimental validation of a PEM fuel cell dynamic model. *Journal of Power Sources*, 173, 310–324.

Dennis, J.E. and Schnabel, J.R.B. (1996). *Numerical Methods for unconstrained optimization and nonlinear equations*. The Society for Industrial and Applied Mathematics.

Karnik, A.Y., Sun, J., Stefanopoulou, A.G., and Buckland, J.H. (2009). Humidity and pressure regulation in a PEM fuel cell using a gain-scheduled static feedback controller. *IEEE transactions on control systems technology*, 17(2), 283–297.

McKay, D., Ott, W., and Stefanopoulou, A. (2005). Modeling, parameter identification, and validation of reactant and water dynamics for a fuel cell stack. In *Proceedings of the IMECE 2005, ASME International Mechanical Engineering Congress*.

Muske, K.R. (1997). Steady-state target optimization in linear model predictive control. In *Proceedings of the American Control Conference*, 3597–3601.

Na, W. and Gou, B. (2008). A thermal equivalent circuit for PEM fuel cell temperature control design. In *Proceedings of the 2008 IEEE International Symposium on Circuits and Systems*, 2825–2828.

O'Rouke, J., Arcak, M., and Ramani, M. (2009). Real-time optimization of net power in a fuel cell system. *J. Power Sources*, 187, 422–439.

Riascos, L.A. and Pereira, D.D. (2009). Optimal temperature control in PEM fuel cells. In *Proceedings of the 35th Annual Conference of IEEE Industrial Electronics*, 2778–2783.

Siegel, J.B. and Stefanopoulou, A.G. (2009). Through the membrane and along the channel flooding in PEMFCs. In *Proceedings of the 2009 American Control Conference*, 2666–2671.

St-Pierre, J., Wilkinson, D., Knights, S., and Bos, M. (2000). Relationshio between water management, contamination and lifetime degration in PEFC. *Journal of New Materials for Electrochemical Systems*, 3, 99–106.